Nanomaterials

International Edition: DOI: 10.1002/anie.201507140
German Edition: DOI: 10.1002/ange.201507140

A Multifunctional Subphthalocyanine Nanosphere for Targeting, Labeling, and Killing of Antibiotic-Resistant Bacteria

*Indranil Roy, Dinesh Shetty, Raghunandan Hota, Kangkyun Baek, Jeesu Kim, Chulhong Kim, Sandro Kappert, and Kimoon Kim**

Dedicated to Professor Nagao Kobayashi

Abstract: *Developing a material that can combat antibiotic-resistant bacteria, a major global health threat, is an urgent requirement. To tackle this challenge, we synthesized a multifunctional subphthalocyanine (SubPc) polymer nanosphere that has the ability to target, label, and photoinactivate antibiotic-resistant bacteria in a single treatment with more than 99 % efficiency, even with a dose as low as 4.2 J cm^{-2} and a loading concentration of 10 nM. The positively charged nanosphere shell composed of covalently linked SubPc units can increase the local concentration of photosensitizers at therapeutic sites. The nanosphere shows superior performance compared to corresponding monomers presumably because of their enhanced water dispersibility, higher efficiency of singlet-oxygen generation, and phototoxicity. In addition, this material is useful in fluorescence labeling of living cells and shows promise in photoacoustic imaging of bacteria in vivo.*

Resistance of bacteria to multiple antibiotics has increased dramatically over the past few years and is currently recognized as a major medical challenge in most healthcare settings.[1] The Center for Disease Control and Prevention has recently issued an assessment that we are very close to entering the "post-antibiotic era",[2] which highlights the need to find innovative and creative solutions to inhibit bacterial growth. Photodynamic therapy (PDT) combines three intrinsically nontoxic components, namely a photosensitizer, light, and oxygen, to generate cytotoxic reactive oxygen species (ROS) and has been proposed as an alternative to controlling bacterial infections.[3] In most cases, although Gram-positive bacteria are susceptible to the photosensitizing action of a variety of sensitizers, Gram-negative bacteria exhibit a remarkable resistance to negatively charged or neutral agents.[4] However, studies shown that cationic photosensitizers can cause direct photoinactivation of Gram-negative bacteria even in the absence of additives.[5] Another promising approach to combating such bacteria is based on nanomaterials, in which the higher number of functional sites compared to any given small molecule enhances the interaction with a given microbe.[6] In spite of progress in this field, however, existing materials have several shortcomings, such as poor water dispersibility and/or nonspecific accumulation of photosensitizers.[7,8] Selective targeting of photosensitizers in microorganisms may solve the problem of nonspecific accumulation and may also reduce the dosage required for PDT. Considering all these aspects, developing a material that possesses the above-mentioned critical criteria would be a great addition to the ongoing fight against the major medical problem of antiobiotic-resistant bacteria.

Subphthalocyanines (SubPcs) have interesting photophysical features, such as intense fluorescence and photosensitizing properties, stemming from their cone-shaped structure and 14-π-electron aromatic conjugated system.[9] In particular, SubPcs have a longer triplet excited-state lifetime compared to other well-known classes of photosensitizers, including porphyrins (Ps) and phthalocyanines (Pcs), which results in a higher quantum yield for the generation of singlet oxygen (0.67 for SubPcs, 0.44 for Ps, and 0.52 for Pcs).[9,10,11b] Additionally, SubPcs show more intense fluorescence signals compared to Ps or Pcs, which may be exploited in efficient fluorescent labeling of living cells. As a result of these merits along with their high phototoxicity and intense light absorption in the therapeutic window ($\lambda = 600$–900 nm), SubPcs have been explored as photosensitizers in PDT.[9] However, these molecules have some serious limitations including limited photostability as well as poor dispersibility in water or phosphate-buffered saline (PBS).[8] To overcome these limitations, we decided to develop well-defined, water-dispersible SubPc-based nanomaterials that can target, label, and photoinactivate antibiotic-resistant bacterial cells. Our strategy involves: 1) synthesis of a hollow nanosphere composed of covalently linked SubPc molecules utilizing the template-free, covalent self-assembly method recently developed by us,[11] which can increase the local concentration of

[*] I. Roy, Dr. D. Shetty, Dr. K. Baek, S. Kappert, Prof. Dr. K. Kim
Center for Self-assembly and Complexity (CSC)
Institute for Basic Science (IBS)
Pohang, 790-784 (Republic of Korea)
E-mail: kkim@postech.ac.kr
Homepage: http://csc.ibs.re.kr/
I. Roy, Dr. R. Hota, Prof. Dr. K. Kim
Department of Chemistry, Pohang University of Science and Technology, Pohang, 790-784 (Republic of Korea)
Prof. Dr. K. Kim
Division of Advanced Materials Science
Pohang University of Science and Technology
Pohang, 790-784 (Republic of Korea)
J. Kim, Prof. Dr. C. Kim
Department of Creative IT Engineering and Electrical Engineering
Pohang University of Science and Technology
Pohang, 790-784 (Republic of Korea)

Supporting information for this article is available on the WWW under http://dx.doi.org/10.1002/anie.201507140.

photosensitizers at therapeutic sites; and 2) introduction of positive charges on the surface of the nanosphere, which enhances their water dispersibility as well as their ability to target negatively-charged bacterial membranes (Figure 1).

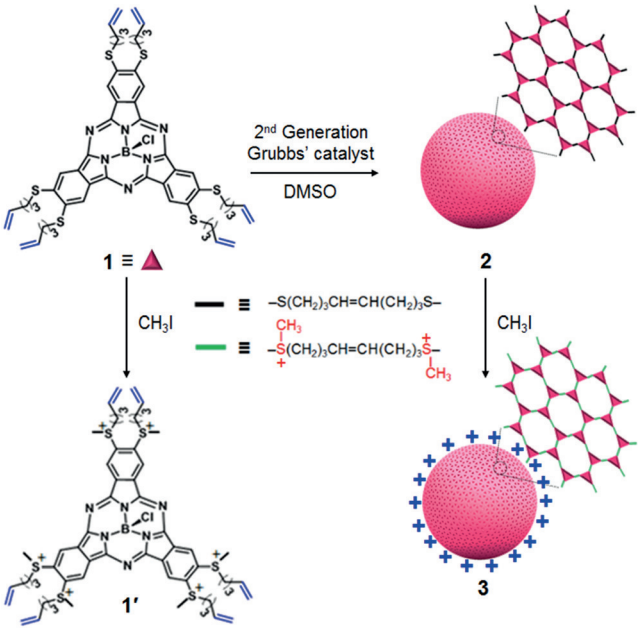

Figure 1. Direct synthesis of SubPc nanosphere **2** from SubPc monomer **1** and its conversion into water-dispersible SubPc nanosphere **3**. The alkylated monomer **1′** was synthesized for control experiments. DMSO = dimethyl sulfoxide.

Herein, we report a stable, water-dispersible, hollow SubPc nanosphere, which is capable of targeting and killing antibiotic-resistant bacteria with exceptional efficiency even at a low dosage upon visible light irradiation. In addition, this nanomaterial is also useful for fluorescent labeling of living cells and shows great promise in photoacoustic imaging of bacteria in vivo.

The SubPc nanosphere **2** was synthesized by an olefin cross-metathesis reaction of monomer **1** without using any templates (Figure 1). In a typical experiment, reaction of **1** (synthesized by means of a seven-step process; see Scheme S1 in the Supporting Information) in DMSO in the presence of 5 mol% of Grubbs catalyst (second generation) at room temperature, followed by dialysis, produced polymer nanosphere **2** (71% yield based on **1**). A combination of scanning electron microscopy (SEM), transmission electron microscopy (TEM), and light-scattering studies confirmed the formation of **2** with an average diameter of 150 ± 30 nm (Figure S4). Furthermore, the FTIR, UV/Vis, and fluorescence spectra of **2** showed characteristic signals of SubPc, confirming that the SubPc core of **1** remain intact in the nanosphere network (Figure S5, S6). We note that the spontaneous formation of a hollow nanosphere from a cone-shaped monomer was a pleasant surprise as covalent self-assembly had previously been achieved only with monomers containing a rigid, flat core.[11]

For in vitro studies, water-dispersible nanosphere **3** was synthesized by treating **2** with methyl iodide followed by dialysis, which resulted in partial alkylation of the thioether units of **2** to convert them into sulfonium groups (Figure 1). There was no significant change in the hydrodynamic size (average diameter 150 ± 30 nm) of **2** even after introducing positive charges onto the surface of the nanosphere. However, the zeta potential of **3** increased to 23 ± 4 mV from 1 ± 3 mV of **2** (Figure S7, S8). This observation indicates that the resulting sulfonium groups are mainly distributed over the surface of **3**. Scanning transmission electron microscopy (STEM) images of **3** showed a very thin shell with an average thickness of 1.0 ± 0.2 nm (Figure 2b, c), indicating that the

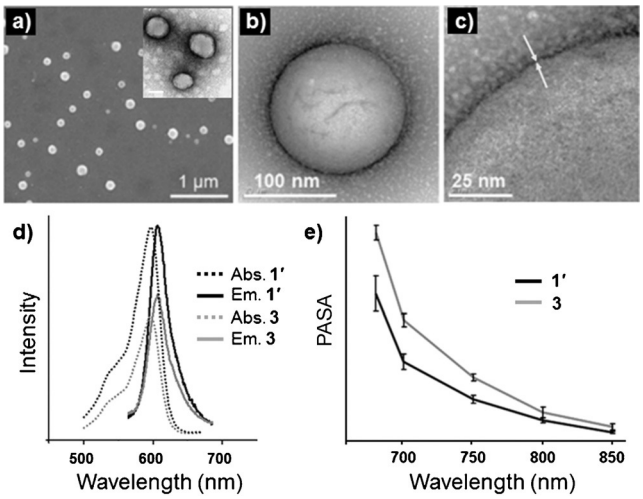

Figure 2. Electron microscopy images of SubPc nanospheres **3**. a) SEM image. Inset in (a): low-resolution TEM image after uranyl acetate staining. b), c) STEM images. d) Absorption and emission spectra of **1′** and **3** in DMSO. e) In vitro photoacoustic properties: spectroscopic photoacoustic signal amplitude (PASA) of **1′** and **3**.

shell is almost one monomer thick (height of the SubPc core = 0.8 nm). The spherical shape of **3** along with the cone-shaped SubPc units effectively prevents aggregation; thus it remains well dispersed in water even after several months (Figure S9). A molecular-mechanics modeling study suggests that the shell of a SubPc nanosphere with a diameter of 150 nm is composed of approximately 18000 SubPc units (Figure S10). Additionally, alkylated SubPc monomer (**1′**) was also synthesized for control experiments (Figure 1).

The absorption and emission spectra of **1′** and **3** are shown in Figure 2d. The absorption spectra of both **1′** and **3** display typical Q bands between $\lambda = 500$ and 630 nm with an absorption maximum at $\lambda_{max} = 600$ nm, characteristic of SubPc. The Q band of nanosphere **3** is somewhat broader compared to monomer **1′** with a lower molar extinction coefficient but essentially the same λ_{max} value, suggesting that photophysically the SubPc units in **3** behave almost like a SubPc monomer. The quantum yields of singlet oxygen generation (SOG) for **3** and **1′** in DMSO are similar (0.7 and 0.68, respectively; measured by using a reported procedure),[12] suggesting that most of the SubPc units of **3** behave as

monomers. However, **3** shows an approximately nine times higher SOG efficiency than **1′** in PBS buffer (0.61 for **3** and 0.07 for **1′**), indicating a much lower propensity for **3** to aggregate in aqueous media.

Several antibiotic-resistant bacterial strains were employed as model biological targets in our studies. Nanosphere **3** with a cationic surface was used to efficiently label *E. coli*, as seen in the microscopy images (Figure 3b). Live-cell imaging was conducted using a fluorescence microscope, with the laser employed for excitation directly into the Q band of **3**. No additional dye molecules were required to achieve labeling of the *E. coli* cells, confirming that **3** could be used as a fluorescent labeling agent for bacteria. The STEM images of *E. coli* bacteria treated with **3** confirm the adhesion of the nanospheres to the surface of bacterial cells (Figure 3c). Moreover, complete rupture of the bacterial membrane was detected after laser irradiation on the nanomaterial-incubated samples (Figure S11). These results suggest that the positively charged surface of **3** promotes its adhesion to the negatively charged bacterial membranes. The subsequent efficient local generation of singlet oxygen destroys the bacterial membranes leading to bacterial cell death.

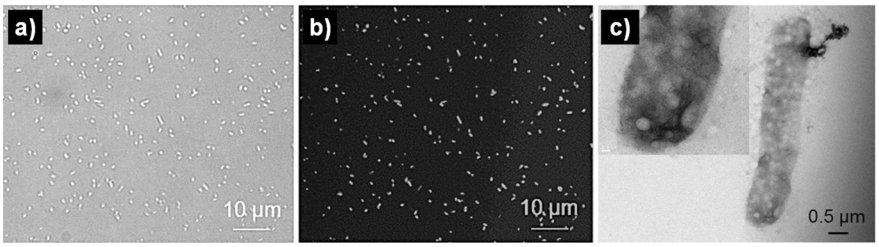

Figure 3. a) Bright-field and b) fluorescence microscopy images of *E. coli* DH5a bacterial cells treated with **3**. c) STEM image (with enlarged portion of the image inset) of *E. coli* DH5a treated with **3** showing the interaction between **3** and the surfaces of the bacterial plasma membranes.

To assess the photobiological activity of **1′** and **3** in more detail, an in vitro study was carried out with different Gram-negative (*E. coli* DH5a and *E. coli* K-12), Gram-positive (*S. aureus* (SA)), and antibiotic-resistant bacterial cells (ampicillin-resistant *E. coli* DH5a (*E. coli* DH5a$_{Amp}$) and methicillin-resistant *S. aureus* (MRSA)). The different bacterial strains were incubated separately with materials **1′** or **3** dispersed in PBS buffer for 30 minutes and the samples were irradiated at $\lambda_{ex} = 600$ nm for a time range between 20 and 120 s (irradiance of 1.4 J cm^{-2} to 8.4 J cm^{-2}). The inactivation of bacterial cells was evaluated by counting the number of colony forming units (CFU) on the Luria broth agar plate (Figure S12). The results of photodynamic inactivation of *E. coli* DH5a and the ampicillin-resistant *E. coli* DH5a after laser irradiation for 60 s are shown in Figure 4. Nanosphere **3** can photoinactivate antibiotic-resistant *E. coli* in a single treatment with more than 99% efficiency even with a dose as low as 4.2 J cm^{-2} and a loading concentration of 10 nM (Figure S13). The minimal bactericidal concentration (MBC) values for **3** and **1′**, which provide valuable information on the potential action of antibacterial agents in vitro, are recorded in Table 1. Interestingly, **3** shows much higher efficiency (ca. 200 times) compared to **1′** for all of the tested bacterial cells at a loading concentration for **3** or **1′** of 10–20 nM and a radiation dose of 4.2 J cm^{-2}. Furthermore, no significant cell death was detected either upon treatment of the cells with **3** without laser irradiation (dark toxicity; Figure 4b, Ctrl 1), or in the absence of **3** but with laser irradiation (Ctrl 2). These results suggest that **3** can efficiently photoinactivate bacterial cells (Figure S13–S15). Remarkably, the dosage used in our studies for efficient photoinactivation is significantly lower (4.2 J cm^{-2}; 60 s) compared to other reported nanomaterials (27 J cm^{-2}; 2 h),[6c] which may have significant clinical implications. We believe that the much higher phototoxicity of **3** compared to **1′** or other nanomaterials is likely due to more efficient interactions with bacterial membranes and a much higher local concentration of $^1O_2$ generated by using **3**.

Interestingly, in addition to the above-described fluorescence signals, strong photoacoustic signals were detected for both **3** and **1′** at $\lambda =$ 680 nm in PBS (Figure 2e). Moreover, the stronger photoacoustic signals generated from **3** than those from **1′** indicated that the heat conversion efficiency of the SubPc nanosphere is higher than that of the SubPc monomer. To explore these

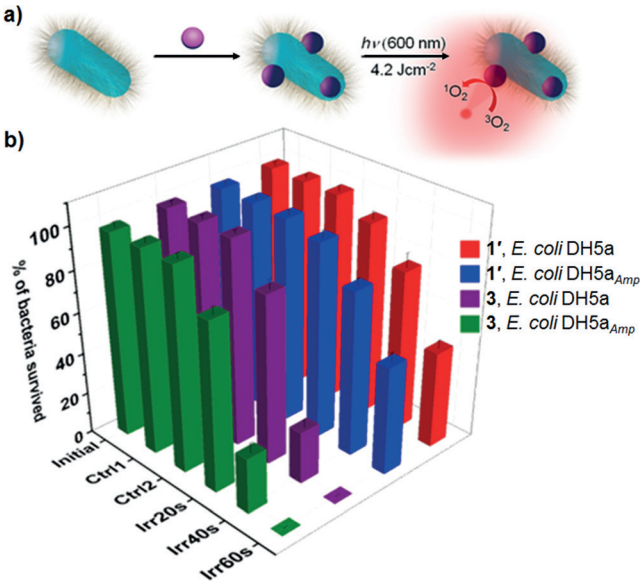

Figure 4. a) Representation of bacterial photoinactivation in the presence of **3**. b) Histogram showing the photodynamic inactivation of *E. coli* DH5a and the ampicillin-resistant strain *E. coli* DH5a$_{Amp}$. Initial: original bacteria count. Ctrl 1: dark toxicity experiments; the bacterial suspension was incubated in the dark with **1′** or **3** dispersed in PBS overnight. Ctrl 2: the bacterial suspension was irradiated with a laser in the absence of photosensitizer. Irr20s, Irr40s, and Irr60s: the bacterial suspension was incubated with **1′** or **3** dispersed in PBS for 30 min and was then irradiated with a laser for 20 s, 40 s, or 60 s, respectively. (An aliquot of 50 μL of a 10 nM solution of **1′** or **3** in PBS was used to inactivate a 150 μL bacterial suspension (10^8 CFU mL^{-1})).

Table 1: Minimal bactericidal concentration (MBC) values of **3** and **1′**.[a]

	E. coli K12	*E. coli* DH5a	*E. coli* DH5a$_{Amp}$	SA	MRSA
3	10 nM	10 nM	10 nM	20 nM	20 nM
1′	2 μM	2 μM	2 μM	4 μM	4 μM

[a] Radiation dose used 4.2 J cm^{-2} (60 s).

properties for bacterial imaging we carried out a preliminary in vivo test using **3**. An aqueous solution of **3** (0.4 mM, 50 μL) was intradermally injected into the bacteria-infected thigh of a rat and photoacoustic images were acquired before and after (60 min) the injection of **3** at $\lambda = 680$ nm. After the injection, distributions of **3** in the bacteria-infected region and bleeding regions caused by the needle insertion were clearly delineated. Most importantly, photoacoustic signals were much stronger in the bacteria-infected region (Figure S18). Similar results were obtained from fluorescence imaging experiments. The fluorescence signal intensity at the infected area after the injection of **3** is significantly higher than that at a control area (Figure S19). Even though further detailed studies are required to confirm the target specificity of **3**, these results suggest another exciting application of **3**, namely in vivo bacterial imaging.[13]

In summary, we have developed a highly stable, water-dispersible, multifunctional SubPc-based nanomaterial that can target, label, and inactivate antibiotic-resistant bacterial cells in a single treatment with more than 99% efficiency. This SubPc hollow nanosphere can be readily synthesized by template-free, covalent self-assembly followed by simple postsynthetic modification. The superior performance of the nanospheres compared to corresponding monomers in the photoinactivation of antibiotic-resistant bacteria is due primarily to its enhanced water dispersibility, higher SOG efficiency, and phototoxicity. The nanosphere is metal free (and thus may have lower toxicity) and can address several other key shortcomings often associated with existing photoactive materials for PDT, such as poor water dispersibility, high dosage requirements, and skin sensitivity.[8,14] Apart from the photodynamic therapeutic benefits, the multifunctional nature of this material may be useful in bacterial imaging in vivo. Incorporation of a covalently linked targeting ligand at the axial position of SubPc units may enhance the chances of target-specific imaging of bacteria. In particular, the photoacoustic properties of our material may render it useful in photoacoustic tomography (PAT) imaging.[15] These results pave the way towards new possibilities for the photodynamic treatment of infectious diseases and the design of next-generation photosensitizers.

Acknowledgements

This work was supported by the Institute for Basic Science (IBS) (IBS-R007-D1). We thank Prof. Dr. W. J. Kim for permitting us using the culture room facility. We also thank Dr. P. Aich and J. Park for useful discussions related to in vitro experiments.

Keywords: antibiotic resistance · nanostructures · photodynamic therapy · self-assembly · subphthalocyanines

How to cite: *Angew. Chem. Int. Ed.* **2015**, *54*, 15152–15155
Angew. Chem. **2015**, *127*, 15367–15370

[1] a) U. Theuretzbacher, *J. Glob. Antimicrob. Resist.* **2013**, *1*, 63–69; b) World Health Organization, **2014**, available at http://www.who.int/mediacentre/news/releases/2014/amr-report/en/.
[2] T. Frieden, Center for Disease Control, **2013**, available at http://www.cdc.gov/drugresistance/threat-report-2013/.
[3] E. Alves, M. A. Faustino, M. G. Neves, A. Cunha, J. Tome, A. Almeida, *Future Med. Chem.* **2015**, *7*, 1221–1224.
[4] M. R. Hamblin, T. Hasan, *Photochem. Photobiol. Sci.* **2004**, *3*, 436–450.
[5] a) D. Lazzeri, M. Rovera, L. Pascual, E. N. Durantini, *Photochem. Photobiol.* **2004**, *80*, 286–293; b) S. Banfi, E. Caruso, L. Buccafurni, V. Battini, S. Zazzaron, P. Barbieri, V. Orlandi, *J. Photochem. Photobiol. B* **2006**, *85*, 28–38.
[6] a) E. Navarro, F. Piccapietra, B. Wagner, F. Marconi, R. Kaegi, N. Odzak, L. Sigg, R. Behra, *Environ. Sci. Technol.* **2008**, *42*, 8959–8964; b) C. N. Lok, C. M. Ho, R. Chen, Q. Y. He, W. Y. Yu, H. Sun, P. K. Tam, J. F. Chiu, C. M. Che, *J. Proteome Res.* **2006**, *5*, 916–924; c) C. A. Strassert, M. Otter, R. Q. Albuquerque, A. Hone, Y. Vida, B. Maier, L. De Cola, *Angew. Chem. Int. Ed.* **2009**, *48*, 7928–7931; *Angew. Chem.* **2009**, *121*, 8070–8073; d) K. Liu, Y. Liu, Y. Yao, H. Yuan, S. Wang, Z. Wang, X. Zhang, *Angew. Chem. Int. Ed.* **2013**, *52*, 8285–8289; *Angew. Chem.* **2013**, *125*, 8443–8447.
[7] L. B. Josefsen, R. W. Boyle, *Br. J. Pharmacol.* **2008**, *154*, 1–3.
[8] M. B. Spesia, E. N. Durantini, *Dye. Pigment.* **2008**, *77*, 229–237.
[9] C. G. Claessens, D. González-Rodríguez, T. Torres, *Chem. Rev.* **2002**, *102*, 835–853.
[10] A. Blum, L. I. Grossweiner, *Photochem. Photobiol.* **1985**, *41*, 27–32.
[11] a) K. Baek, I. Hwang, I. Roy, D. Shetty, K. Kim, *Acc. Chem. Res.* **2015**, *48*, 2221–2229; b) R. Hota, K. Baek, G. Yun, Y. Kim, H. Jung, K. M. Park, E. Yoon, T. Joo, J. Kang, C. G. Park, S. M. Bae, W. S. Ahn, K. Kim, *Chem. Sci.* **2013**, *4*, 339–344; c) D. Kim, E. Kim, J. Kim, K. M. Park, K. Baek, M. Jung, Y. H. Ko, W. Sung, H. S. Kim, J. H. Suh, C. G. Park, O. S. Na, D. K. Lee, K. E. Lee, S. S. Han, K. Kim, *Angew. Chem. Int. Ed.* **2007**, *46*, 3471–3474; *Angew. Chem.* **2007**, *119*, 3541–3544.
[12] W. Spiller, H. Kliesch, D. Wohrle, S. Hackbarth, B. Roder, G. Schnurpfeil, *J. Porphyrins Phthalocyanines* **1998**, *2*, 145–158.
[13] a) X. Ning, S. Lee, Z. Wang, D. Kim, B. Stubblefield, E. Gilbert, N. Murthy, *Nat. Mater.* **2011**, *10*, 602–607; b) M. van Oosten, T. Schäfer, J. A. C. Gazendam, K. Ohlsen, E. Tsompanidou, M. C. de Goffau, H. J. M. Harmsen, L. M. A. Crane, E. Lim, K. P. Francis, L. Cheung, M. Olive, V. Ntziachristos, J. M. van Dijl, G. M. van Dam, *Nat. Commun.* **2013**, *4*, 2584–2591.
[14] a) T. S. Mang, T. J. Dougherty, W. R. Potter, D. G. Boyle, S. Somer, J. Moan, *Photochem. Photobiol.* **1987**, *45*, 501–506; b) B. Petersen, S. R. Wiegell, H. C. Wulf, *Br. J. Dermatol.* **2014**, *171*, 175–178.
[15] C. Kim, C. Favazza, L. V. Wang, *Chem. Rev.* **2010**, *110*, 2756–2782.

Received: July 31, 2015
Published online: October 23, 2015

